

A time-dependent approach to the kinetics of homogeneous nucleation

Terry Olson and Patrick Hamill

Physics Department, San Jose State University, 1 Washington Square, San Jose, California 95192

(Received 29 August 1995; accepted 27 September 1995)

We present a time-dependent model for homogeneous nucleation and derive a time-dependent solution to the coupled growth-rate equations for molecular cluster concentrations. A correction to the monomer concentration growth-rate equation is applied, which accounts for the gain and loss of molecules by all cluster populations. The condensation rate used considers all embryos to be in motion, rather than assuming that only the monomers move. In order to allow for size-dependent variations in a cluster's surface tension, the evaporation rate incorporates the revised parametrization of Laaksonen *et al.* [Phys. Rev. E **49**, 5517 (1994)] of the homogeneous nucleation theory of Dillmann and Meier [J. Chem. Phys. **94** 3872 (1991)]. Eigenvalue analysis illuminates how the steady-state is approached from the transient period and allows us to estimate the accuracy of a steady-state approximation. It is shown that the distributions of clusters predicted by this theory generate nucleation currents that are more accurate than those produced by other steady-state cluster distributions. More importantly, this model can be used to calculate the time-dependent cluster behavior for any nucleation model that has an expression for the change in Gibbs free energy. The theory agrees well with the experimental data of Miller *et al.* [J. Chem. Phys. **78**, 3204 (1983)] and Viisanen *et al.* [J. Chem. Phys. **99** 4680 (1993)], and with the theoretical predictions of Laaksonen *et al.* © 1996 American Institute of Physics. [S0021-9606(96)01901-5]

I. INTRODUCTION

Nucleation is the thermodynamic molecular process that initiates many phase transitions. We observe nucleation events on a day-to-day basis, some examples being cloud creation (the formation of liquid droplets within a vapor), making ice (the formation of solid crystals within a liquid), and boiling water (the formation of gaseous bubbles within a liquid). There is a strong motivation to study nucleation because phase transitions are pervasive in many important physical phenomena. In homogeneous nucleation, the nucleating substance and its environment are assumed pure; there are no foreign particles, such as dust, wall surfaces, or ions, that can serve as sites for the onset of the phase change. Consequently, of all the nucleation theories, homogeneous nucleation is the simplest. Its simplicity does not undermine its significance, however, as its concepts are applied by many theorists to explain more complicated processes.

The classical approach to homogeneous nucleation was originated and developed by Becker and Döring,¹ Farkas,² Frenkel,³ Volmer and Weber,⁴ and Zeldovich;⁵ an excellent two-part review is given by McDonald.^{6,7} The theory focuses on the vapor-to-liquid phase transition and attempts to calculate the time-independent rate of droplet formation within a given volume of vapor; this rate is called the steady-state nucleation current. Molecular clusters are allowed to change size only by gaining and losing single molecules (monomers) by condensation and evaporation. It is important to note that for a vapor-to-liquid transition, homogeneous nucleation will take place only if the vapor is supersaturated. In other words, the ratio of the vapor pressure to the saturation vapor pressure must be greater than one; this ratio is called the supersaturation ratio, and the saturated vapor pressure is defined as the pressure of a saturated vapor over a plane liquid surface.

Thermodynamically, the growth of a droplet is assumed to be governed by the change in Gibbs free energy, which classically has two terms: the first is the bulk energy of liquid phase formation, which is negative and varies as the droplet's volume; the second is the surface free energy, which is positive and varies as the droplet's surface area. For very small molecular clusters, the surface energy dominates the bulk energy, but for larger clusters the bulk energy becomes dominant. Therefore, the Gibbs free energy curve is initially steep and increasing, but as a molecular cluster (an embryo) grows, the curve reaches a maximum and then decreases, the rate of descent growing as the cluster gets larger (Fig. 1 depicts a modified version of this curve). Because a thermodynamic system will spontaneously tend to go to the lowest Gibbs free energy state, the maximum in the curve serves as an activation barrier. Unless an embryo becomes large enough to overcome this barrier, it will tend to decrease its Gibbs free energy by losing molecules by evaporation. The cluster size at which the activation barrier occurs is called the critical size. Because the Gibbs curve is at a maximum, the critically sized cluster is at an unstable equilibrium with respect to the supersaturated vapor. In other words, the vapor is saturated with respect to the surface of the embryos at the critical size. Furthermore, the vapor is supersaturated with respect to the surfaces of supercritically sized clusters and subsaturated with respect to the surfaces of subcritically sized clusters. This explains the tendency of supercritical embryos to grow and subcritical embryos to shrink.

The classical theory of homogeneous nucleation uses the Gibbs free energy to calculate the time-independent distribution of embryos for a supersaturated vapor constrained to be in complete thermodynamic equilibrium; this is called the "balanced steady state" and is characterized by a steady-state nucleation current equal to zero. The constrained equi-

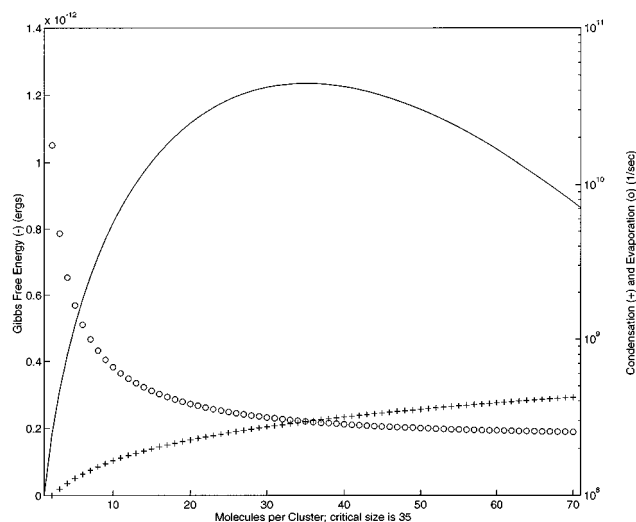


FIG. 1. The Gibbs free energy, as modified by Laaksonen *et al.* (Ref. 14), is compared with the rates of condensation and evaporation for water vapor having a supersaturation ratio of 10.52 at 248.45 K.

librium distribution of embryos is a mathematical artifice. The balanced steady state is nonphysical for a supersaturated vapor because a supersaturated vapor is not in complete thermodynamic equilibrium and, therefore, produces a nonzero current.

Simple kinetic arguments are employed by the classical theory to obtain a time-independent rate of the number of monomers condensing onto a motionless embryo. This condensation rate is combined with the constrained equilibrium distribution to derive the rate at which molecules evaporate from a given cluster. The classical theory then applies the condensation and evaporation rates to derive the size-dependent currents, each of which is the net number of embryos becoming one molecule larger in a given time and volume. These currents represent the total flow of embryos between concentrations of molecular clusters.

At this point in the classical theory two crucial assumptions are made. The first assumption is that a steady-state period exists during nucleation in which the concentrations of equally sized embryos remain constant. Consequently, the currents between the embryo concentrations must all have equal magnitudes; a concentration of clusters could not be constant if the rate of embryos flowing "in" were not equal to the rate flowing "out." The distribution of cluster concentrations during the steady-state period is called the steady-state distribution. Since the currents all have the same magnitude, they lose their size dependence and are considered to be the steady-state current. This steady-state current is taken to be the nucleation rate. The second assumption is that the time it takes for the embryo concentrations to initially grow and form the steady-state distribution is negligible when compared to the steady-state period; this initial period of time is called the transient period. Thus, the entire homogeneous nucleation process is modeled with only the steady-state period in consideration.

Removing the time dependence of the cluster concentra-

tions considerably simplifies the mathematics of the classical theory. When the previous two assumptions have been made, it is not difficult to obtain the value of the steady-state nucleation current. The classical theory usually concludes with this calculation.

At first, experimentalists found the agreement between the classical theory and experiment to be generally good.⁸⁻¹⁰ Unfortunately, they were not measuring nucleation rates; they were measuring the supersaturation ratios at which the steady-state current was equal to one droplet formed per cubic centimeter per second. The classical theory agreed with these measurements. In the last two decades, however, it has become possible to measure actual nucleation rates. New experimental data¹¹⁻¹³ has shown that in the case of water, the classical theory's agreement is limited to small currents. As the currents and supersaturation ratios become larger in magnitude, the theoretical agreement worsens, the predictions being consistently too high. Furthermore, the observed temperature dependence of nucleation rates is weaker than that which is predicted.

There are many possible shortcomings in the classical theory of homogeneous nucleation, and the motivation to find a more suitable approach is clear. One such defect is the omission of the transient period. By assuming this time to be insignificant, and thereby immediately placing the embryos into their steady-state distribution, one cannot obtain time-dependent expressions for either the cluster concentrations or the currents between them. Using a nonclassical semiphenomenological approach, Laaksonen *et al.*¹⁴ developed a revised version of the steady-state nucleation rate theory of Dillmann and Meier¹⁵ that agrees with experimental data for many different substances over a wide range of temperatures. As with the classical theory, however, they have not produced an expression that includes the time dependence of the individual cluster concentrations. The utility of considering this time evolution has been demonstrated by Abraham¹⁶ and Wilcox and Bauer.¹⁷ Abraham found that during the transient period, the currents between concentrations of embryos smaller than the critical size were at times much larger than the steady-state current; these currents significantly changed in magnitude even when the corresponding concentrations were almost steady. Neither he nor Wilcox and Bauer obtained time-dependent expressions, however, but generated time evolution plots by numerically integrating the necessary growth-rate differential equations.

In this paper, it is our goal to present a time-dependent expression for cluster concentrations within the context of homogeneous nucleation. The theoretical derivation is general and may be applied to different substances. We incorporate the kinetic theory of dilute vapors to obtain a condensation rate that assumes all of the embryos are in motion; this is in contrast to the standard technique of assuming that only the monomers move. The Laaksonen *et al.* reparametrization of the Dillmann and Meier homogeneous nucleation theory is then employed to derive the evaporation rate. Using the conservation of mass, we correct the standard monomer concentration growth-rate equation, which can be shown to be erroneous. Finally, the entire system of cluster concentration

growth-rate equations is solved using matrix methods.

The advantages of this time-dependent approach are many. This model allows us to calculate the time-dependent behavior of embryos for almost any homogeneous nucleation theory; an expression for the change in Gibbs free energy is all that is required. We are able to predict how many embryos of a particular size are present at a given time for any supersaturation ratio and temperature. It then becomes clear how the thermodynamic system approaches the steady-state from its transient period of growth. Furthermore, the time-dependent expressions allow us to determine the relative accuracy of the steady-state approximation, and to calculate when each individual embryo number concentration slows its growth enough to be considered steady. The predicted nucleation currents are in excellent agreement with experimental data and the results predicted by Laaksonen *et al.*¹⁴

II. DERIVING THE RATES OF CONDENSATION AND EVAPORATION

We begin our analysis of the nucleation of droplets by restricting the ways which a molecular cluster may increase or decrease in size. During nucleation the number of monomers in the supersaturated vapor is significantly larger than the total number of clusters (dimers, trimers, etc.). It is reasonable then to assume that the only way a cluster becomes larger or smaller is by gaining or losing single molecules. Let x be a discrete variable representing the number of molecules in an embryo. An embryo consisting of x molecules (an “ x -mer”) is denoted A_x . It increases its size by gaining a single molecule A_1 ,



and decreases its size by losing a molecule,



Of course, it is possible for an x -mer to absorb a dimer, trimer, or any other embryo; the frequency of such an event, however, is negligible compared to monomer absorption. Assuming that only binary collisions take place is essentially the same as assuming that the supersaturated vapor is dilute. (Even for a supersaturation of 10.52 and a temperature of 248.45 K, which corresponds to a nucleation rate of 100 million droplets/cc/sec,¹³ the maximum cluster diameter is only 6.5% of the mean molecular spacing of monomers within the vapor.) Reactions (1) and (2) are starting points for many theoretical approaches to homogeneous nucleation. It has been suggested that the formation of dimers involves three molecules, as opposed to two,¹⁸ the involvement of the third molecule is a consequence of the conservation of energy and momentum. This use of an additional reactant might also be necessary for slightly larger clusters;¹⁷ however, it is most likely to be a neutral component, such as a carrier gas molecule. For the sake of simplicity, we will maintain the assumption that clusters grow and shrink only by gaining and losing monomers.

An x -mer gains and loses molecules by condensation and evaporation. The rates at which molecules condense onto and evaporate off of an x -mer in a given time interval are denoted c_x and e_x , respectively.

We use four fundamental assumptions to obtain a numerical expression for c_x . First, we assume that all x -mers are spherical; this approximation naturally loses accuracy as the embryos get smaller. Second, we attribute the density of the liquid phase, ρ , to each of the x -mers. These two assumptions can be summarized by the equation

$$\frac{4}{3} \pi r_x^3 \rho = m_1 x, \quad (3)$$

where m_1 represents the mass of one molecule and r_x represents the radius of the x -mer. The third and fourth assumptions are that the number of monomers per unit volume, n_1 , and the temperature of the vapor, T , are constant during the nucleation period. Of course, the monomer concentration must be depleted for molecular clustering to take place, but we assume that this depletion is insignificant.

We obtain the condensation rate by evaluating the rate of molecular collisions using the kinetic theory of dilute vapors. This approach is advantageous because all embryos are considered to be in motion. (The classical treatment of condensation assumes that the embryos are suspended at rest in the vapor, with the monomers being the only moving bodies.) We treat the vapor as a gas mixture, each gas containing all of the embryos which have the same number of molecules. If a collision between a monomer and an x -mer occurs, the distance between the centers of the two, r_{x1} , must be

$$r_{x1} = r_x + r_1. \quad (4)$$

Using Eq. (3),

$$r_{x1} = \left(\frac{3m_1 x}{4\pi\rho} \right)^{1/3} + \left(\frac{3m_1}{4\pi\rho} \right)^{1/3} = \left(\frac{3m_1}{4\pi\rho} \right)^{1/3} (x^{1/3} + 1). \quad (5)$$

Envision a shell with radius r_{x1} surrounding the x -mer. Whenever the center of a monomer intersects this shell, the x -mer and monomer collide. The cross-sectional area of the shell is the total collision cross section and is denoted by α_{x1} , where

$$\alpha_{x1} = \pi r_{x1}^2. \quad (6)$$

Consider an x -mer moving with velocity \mathbf{v}_x through a vapor of randomly moving monomers. Given the monomer number density at time t , $n_1(t)$, a small number $\Delta n_1(t)$ will have velocities within the interval $[\mathbf{v}, \mathbf{v} + \Delta \mathbf{v}]$. We choose a reference frame in which these monomers are at rest and the x -mer has the relative velocity $\mathbf{v}_{r_{x1}}$, where

$$\mathbf{v}_{r_{x1}} = \mathbf{v}_x - \mathbf{v}. \quad (7)$$

In time Δt , the x -mer, moving with velocity $\mathbf{v}_{r_{x1}}$ and having the total collision cross section α_{x1} , sweeps out a cylinder of volume $\alpha_{x1} v_{r_{x1}} \Delta t$. The chance that an x -mer moving with velocity \mathbf{v}_x collides with a monomer having a velocity in the range $[\mathbf{v}, \mathbf{v} + \Delta \mathbf{v}]$ is $\Delta n_1(t) \alpha_{x1} v_{r_{x1}} \Delta t$. This corresponds to a collision frequency of $f_v(t)$,

$$f_\nu(t) = \Delta n_1(t) \alpha_{x1} \nu_{r_{x1}}. \quad (8)$$

The total collision frequency, which is the mean rate of collisions between the x -mer and the monomers, is obtained by summing $f_\nu(t)$ over all of the possible monomer speeds:

$$\begin{aligned} f_{x1}(t) &= \sum_\nu f_\nu(t) \\ &= \sum_\nu \Delta n_1(t) \alpha_{x1} \nu_{r_{x1}} \\ &= n_1(t) \alpha_{x1} \sum_\nu \frac{\Delta n_1(t)}{n_1(t)} \nu_{r_{x1}}. \end{aligned} \quad (9)$$

Note that $\Delta n_1(t)/n_1(t)$ is the fraction of monomers having a velocity in the range $[\nu, \nu + \Delta\nu]$, so the summation in the last term of Eq. (9) is equal to the mean value of $\nu_{r_{x1}}$. Thus,

$$f_{x1}(t) = n_1(t) \alpha_{x1} \langle \nu_{r_{x1}} \rangle. \quad (10)$$

One of our fundamental assumptions was that the number density of monomers was time independent,

$$n_1(t) \approx n_1(0). \quad (11)$$

This assumption removes the time dependence from the total collision frequency, hence

$$f_{x1} = n_1(0) \alpha_{x1} \langle \nu_{r_{x1}} \rangle. \quad (12)$$

From basic kinetic theory for a hard-sphere molecule gas at equilibrium,¹⁹

$$\langle \nu_{r_{x1}} \rangle = \left(\frac{8kT}{\pi m_r} \right)^{1/2}, \quad (13)$$

where m_r is the reduced mass,

$$m_r = \frac{m_1 m_x}{m_1 + m_x} = \frac{m_1 (x m_1)}{m_1 + x m_1} = \frac{x m_1}{1 + x}. \quad (14)$$

Using Eqs. (5), (6), (12), (13), and (14), we obtain a useful expression of the total collision frequency,

$$f_{x1} = \beta n_1(0) (x^{1/3} + 1)^2 \left(\frac{x+1}{x} \right)^{1/2}, \quad (15)$$

where

$$\beta \equiv \left(\frac{3m_1}{4\pi\rho} \right)^{2/3} \left(\frac{8\pi kT}{m_1} \right)^{1/2}. \quad (16)$$

Let us define the sticking coefficient ϕ_x as the probability that a monomer hitting an x -mer sticks to it. The product of ϕ_x and f_{x1} yield a rate at which monomers hit and stick to an x -mer; this is the condensation rate c_x ,

$$c_x = \phi_x \beta n_1(0) (x^{1/3} + 1)^2 \left(\frac{x+1}{x} \right)^{1/2}. \quad (17)$$

We will assume that ϕ_x is equal to unity, so all molecules that collide with an embryo stick to it.

One might be opposed to treating the supersaturated vapor as being at equilibrium in the derivation of Eq. (13). When a vapor is in an equilibrium state the number of mol-

ecules in any velocity class is time independent, so during the steady-state period, when fluctuations of the embryo concentrations are small, the vapor is at a quasiequilibrium. In fact, we have already assumed a quasiequilibrium by assigning a single temperature to the vapor.

In the spirit of Katz and Wiedersich,²⁰ we derive the evaporation rate e_x by considering the equilibrium number density of x -mers, n_x^E , in a *saturated* vapor. This approach differs from the classical theory, which invokes a *supersaturated* vapor constrained to be in equilibrium.

The equilibrium concentration for x -mers is usually written in the form

$$n_x^E = n_1^E \exp\left(\frac{-\Delta G_x}{kT} \right), \quad (18)$$

where ΔG_x is the change in the Gibbs free energy of formation of an x -mer. The net flow of embryos per unit time per unit volume from the x -mer concentration, $n_x(t)$, to the $(x+1)$ -mer concentration, $n_{x+1}(t)$, is defined as the nucleation current, $I_x(t)$,

$$I_x(t) \equiv c_x n_x(t) - e_{x+1} n_{x+1}(t). \quad (19)$$

Homogeneous nucleation cannot occur in a saturated vapor, which is in equilibrium with a plane surface of the liquid phase; this means essentially that the critically sized cluster within a saturated vapor must be infinitely large. Hence, the number densities of x -mers are time independent and the nucleation currents between the concentrations of embryos are equal to zero. Using Eq. (19),

$$0 = c_x^{(S=1)} n_x^E - e_{x+1} n_{x+1}^E, \quad (20)$$

where $c_x^{(S=1)}$ corresponds to the condensation rate of a saturated vapor. The evaporation rate is then simply expressed as

$$e_x = c_{x-1}^{(S=1)} \frac{n_{x-1}^E}{n_x^E}. \quad (21)$$

Using Eq. (18),

$$e_x = c_{x-1}^{(S=1)} \exp\left(\frac{\Delta G_x - \Delta G_{x-1}}{kT} \right). \quad (22)$$

It remains to obtain formulas for the Gibbs free energy terms in Eq. (22). There have been many theoretical approaches to determining the Gibbs free energy of a homogeneously nucleating embryo,²¹ however, an expression that works for all substances under all possible conditions has not yet been found. We choose to use an approach developed by Ford *et al.*²² and Laaksonen *et al.*¹⁴ in which the Dillmann and Meier theory is revised; this method agrees with experimental data for n -nonane, water, and the lower alcohols. In brief, we will derive the Ford *et al.* expression for steady-state cluster populations, impose a condition posed by Laaksonen *et al.*, and apply this modified expression to a saturated vapor. The result will be combined with a condensation rate in order to obtain the evaporation rate.

We begin by using an expression for the equilibrium population of clusters within a supersaturated vapor,¹⁵

$$N_x^E = \exp\left(-K_x \theta x^{2/3} - \tau \ln x + \ln(q_0 V) + x \frac{\Delta\mu}{kT}\right). \quad (23)$$

The function K_x describes the surface energy deviations of an x -mer from the surface energy of a macroscopic liquid droplet; τ and q_0 are parameters related to the configurational effects of the embryo as well as its rotational, vibrational, and translational degrees of freedom; the term θ is given by

$$\theta \equiv \frac{\sigma}{kT} \left(\frac{6m_1(\pi)^{1/2}}{\rho}\right)^{2/3}, \quad (24)$$

in which σ is the surface tension of a macroscopic liquid droplet at temperature T , V is the volume occupied by the vapor, and $\Delta\mu$ is the difference between the chemical potentials of a supersaturated and saturated vapor. Assuming that the partial pressure of the monomers is approximately equal to the total vapor pressure, we can express this difference in chemical potentials as²³

$$\Delta\mu \approx kT \ln(S) + B(p - p_\infty) + O(S^2), \quad (25)$$

where the last term denotes truncation error and B is the second virial coefficient from the virial equation of state, in the form

$$pV \left/ \sum_{i=1}^{\infty} iN_i^E = kT + \sum_{j=1}^{\infty} B_j p^{j-1} \right. \quad (26)$$

Using Eqs. (23) and (25), we obtain an expression for the equilibrium cluster populations,

$$N_x^E = S^x \exp\left(-K_x \theta x^{2/3} - \tau \ln x + \ln(q_0 V) + x \frac{B(p - p_\infty)}{kT}\right). \quad (27)$$

In order to obtain an expression for K_x , the surface energy modification, we will use a truncated form of the virial equation of state,

$$\frac{pV}{N_1^E + 2N_2^E} \approx kT + Bp. \quad (28)$$

This may be rewritten as

$$kT + Bp \approx \frac{pV}{N_1^E [1 + 2(N_2^E/N_1^E)]} \approx \frac{pV}{N_1^E} [1 - 2(N_2^E/N_1^E)]. \quad (29)$$

Substituting Eq. (27) into Eq. (29), and using the fact that

$$\frac{Bp}{kT} \ll 1, \quad (30)$$

we reexpress the virial equation of state as

$$kT + Bp \approx \frac{p_\infty}{q_0} \exp\left(K_1 \theta + \frac{Bp_\infty}{kT}\right) \left[1 - \frac{Bp}{kT} - S \times \exp\left(\theta(K_1 - K_2 2^{2/3}) - (\tau - 1) \ln 2 - \frac{Bp_\infty}{kT}\right)\right]. \quad (31)$$

Compare terms to obtain the values of K_1 and K_2 :¹⁴

$$K_1 = \frac{-1}{\theta} \left[\ln\left(\frac{p_\infty}{q_0 kT}\right) + \frac{Bp_\infty}{kT} \right] \quad (32)$$

and

$$K_2 = \frac{-1}{\theta 2^{2/3}} \ln\left[\frac{-Bp_\infty}{kT} 2^\tau \exp\left(-K_1 \theta + \frac{Bp_\infty}{kT}\right)\right]. \quad (33)$$

K_x is expanded in powers of $x^{-1/3}$ (which corresponds to $1/r_x$)

$$K_x = 1 + a_1 x^{-1/3} + a_2 x^{-2/3}, \quad (34)$$

where a_1 and a_2 are determined by Eq. (34) for x equal to 1 and 2,

$$a_1 = \frac{(K_2 - K_1 2^{-2/3}) + 2^{-2/3} - 1}{2^{-1/3} - 2^{-2/3}}, \quad (35)$$

and

$$a_2 = K_1 - 1 - a_1. \quad (36)$$

Note that a_1 is independent of the quantity q_0 , since

$$K_2 - K_1 2^{-2/3} = \frac{-1}{\theta 2^{2/3}} \left[\ln\left(\frac{-Bp_\infty}{kT} 2^\tau\right) - \frac{Bp_\infty}{kT} \right] \approx \frac{-1}{\theta 2^{2/3}} \ln\left(\frac{-Bp_\infty}{kT} 2^\tau\right). \quad (37)$$

This q_0 independence was first noted by Ford *et al.*²² Neglecting the second virial coefficient term in Eq. (27), as it is numerically insignificant [Eq. (30)], we obtain Ford *et al.*'s expression for the equilibrium population of x -mers,

$$N_x^E = N_1^E \exp\{-\theta[x^{2/3} + a_1 x^{1/3} - (a_1 + 1)] - \tau \ln x + (x - 1) \ln S\}. \quad (38)$$

Laaksonen *et al.*¹⁴ considered τ in Eq. (38) to be a theoretical free parameter, removing its original dependence¹⁵ on experimentally measurable values; they determined that setting τ equal to zero produced the best fit with nucleation data for n -nonane, water, and the lower alcohols. Thus we arrive at their expression for the change in an x -mer's Gibbs free energy by considering Eq. (18),

$$\Delta G_x^{(L)} = kT \theta [x^{2/3} + a_1 x^{1/3} - (a_1 + 1)] - kT(x - 1) \ln S. \quad (39)$$

We now obtain the evaporation rate by combining Eqs. (39) and (22) with the saturation ratio equal to one,

$$e_x = c_{x-1}^{(S=1)} \exp\{\theta[x^{2/3} - (x - 1)^{2/3} + a_1 x^{1/3} - a_1(x - 1)^{1/3}]\}, \quad (40)$$

where, using Eq. (17),

$$c_{x-1}^{(S=1)} = \phi_{x-1} \beta [n_1^{(S=1)}(0)] [(x - 1)^{1/3} + 1]^2 \left(\frac{x}{x - 1}\right)^{1/2}. \quad (41)$$

Equations (41) and (17) require formulas for the initial monomer concentrations of a saturated and supersaturated vapor; these can be obtained using Eqs. (27) and (32),

$$n_1(0) = \frac{p}{kT} \left(1 + \frac{Bp}{kT} \right). \quad (42)$$

Note that e_x is independent of the supersaturation ratio of the nucleating vapor, but is sensitive to the embryo size, vapor temperature, and surface tension [see also Eq. (24) for surface tension and temperature terms within θ]. e_x is also undefined for $x=1$, as it should be, since a monomer cannot evaporate.

The relationship of c_x and e_x to the Gibbs free energy is shown in Fig. 1. Note that the condensation and evaporation rates are equal when the free energy curve reaches its maximum; the cluster size at which this occurs is denoted the critical size, x_C . For x -mers smaller than the critical size, the slope of the Gibbs free energy curve is positive; accordingly, the evaporation rate dominates over the condensation rate. On the other hand, for x -mers larger than the critical size, the slope of the Gibbs free energy curve is negative and the condensation rate dominates over the evaporation rate. This behavior is in agreement with the fact that thermodynamic systems tend to spontaneously assume the lowest possible state of Gibbs free energy. Embryos smaller than the critical size tend to shrink by evaporation while those larger than the critical size tend to grow by condensation.

III. DISCUSSION OF THE EMBRYO GROWTH-RATE EQUATIONS WITH A CORRECTION FOR THE MONOMERS

Having deduced the mechanisms by which a cluster increases and decreases in size, we can derive the growth-rate equation for the concentration of x -mers at time t , $n_x(t)$. An x -mer is created when either an $(x-1)$ -mer grows by condensation or when an $(x+1)$ -mer shrinks by evaporation. However, an x -mer is destroyed when it grows by condensation or shrinks by evaporation. Hence,

$$\begin{aligned} \frac{d}{dt} n_x(t) = & c_{x-1} n_{x-1}(t) - (c_x + e_x) n_x(t) \\ & + e_{x+1} n_{x+1}(t) \quad \text{for } x \geq 2, \end{aligned} \quad (43a)$$

where the first and third terms on the right represent the inflow of clusters entering $n_x(t)$ (x -mer creation) while the second term on the right represents the outflow (x -mer destruction). Note that this is a simple inflow-outflow ordinary differential equation for the time rate of change of each embryo concentration (dimers, trimers, etc.). It is convenient to reexpress this growth-rate equation using the definition of the nucleation current, Eq. (19),

$$\frac{d}{dt} n_x(t) = I_{x-1}(t) - I_x(t) \quad \text{for } x \geq 2. \quad (43b)$$

The entire nucleating system (except the monomers) can be represented by a set of coupled differential equations in the form of Eqs. (43a) or (43b). This set has a lower bound, the dimer concentration $n_2(t)$; the growth rate equation for the monomer concentration will be addressed later. Because of the forward coupling in Eq. (43a), we cannot mathematically solve the coupled set unless it has an upper bound, i.e.,

a maximum finite value for the cluster size x . A common technique is to choose some size, G , that is about twice the critical size; clusters having this many molecules are assumed to simply keep growing, assuming a negligible chance to shrink from evaporation. Some treatments effectively remove the G -mers from the system by invoking the Szilard boundary condition, in which the G -mer population is set to zero, decomposed into separate molecules, and then inserted back into the monomer population.⁷

Another approach is to define G as an absorbing state,²⁴ in which case embryos are not allowed to leave the $n_G(t)$ concentration once they have entered it,

$$c_G = e_G = 0. \quad (44)$$

By setting c_G equal to zero, the absorption condition terminates the forward coupling of the growth-rate equations, giving them an upper bound,

$$\frac{d}{dt} n_G(t) = c_{G-1} n_{G-1}(t). \quad (45)$$

The absorbing state is assumed to be so large that its embryos will just keep growing, thus e_G is set equal to zero. This method differs from the Szilard method because the G -mers remain in the system, they are not removed. Note that both methods treat the $n_{x < G}(t)$ populations in the same manner. The growth-rate equation for $n_{G-1}(t)$ has no contribution from the G -mers,

$$\frac{d}{dt} n_{G-1}(t) = c_{G-2} n_{G-2}(t) - (c_{G-1} + e_{G-1}) n_{G-1}(t). \quad (46)$$

In this study we decided to use the absorbing state method for two reasons. First, by not setting the number of G -mers to zero, we can check that our model is conserving mass by confirming that the total number of molecules remains constant. Secondly, the absorbing state method is advantageous because it allows us to determine approximately when the first G -mer is formed.

The formation of the first G -mer is important because it occurs at the maximum time for which the growth rate equations are completely accurate. As long as there are no G -mers, Eq. (46) is physically realistic. However, as soon as the first cluster occupies the absorbing state there is a chance that it will lose a molecule by evaporation. This probability is smaller than the chance of growth by condensation, but it should not be neglected, regardless of the absorption condition, Eq. (44). In fact, the difference between e_2 and c_2 is usually much larger than that between c_G and e_G (if they are not set to zero), yet we do not consider c_2 negligible because embryos would be unable to grow beyond the dimer state (see Fig. 1). Therefore, once the absorbing state is first populated, Eq. (46) loses accuracy since it lacks the evaporation contribution to $n_{G-1}(t)$ from the G -mers. Consequently, the calculated growth rate for $n_{G-1}(t)$ is smaller than its true value. This causes the calculated value of the $(G-1)$ -mer concentration to also be smaller, and the error propagates to all of the embryo concentrations through the backwards coupling of the growth-rate equations (43a). It has been shown,

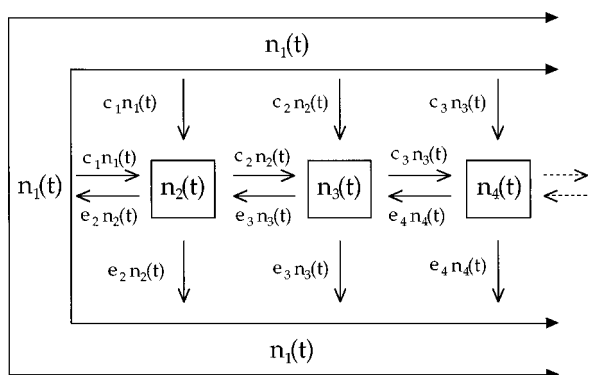


FIG. 2. The growth rate of the monomer concentration is affected by the growth and decay of all the embryo concentrations. For example, when $c_2 n_2(t)$ dimers become trimers, $n_1(t)$ loses $c_2 n_2(t)$ monomers.

however, that the nucleation rate is only slightly affected by the value chosen for G ;⁷ therefore the inaccuracy in the growth-rate equations is small, and we will use the absorption condition, Eq. (44), regardless of the slight error. Note that the Szilard boundary condition also introduces this inaccuracy by setting $n_G(t)$ to zero.

One might be tempted to keep e_G equal to its calculated value, instead of setting it to zero, in order to maintain the accuracy of the $n_{G-1}(t)$ concentration. This, however, produces significant errors into the model, resulting in negative currents which deter the concentrations from their steady state. In other words, the unrealistically large G -mer concentration causes $e_G n_G(t)$ to dominate $c_{G-1} n_{G-1}(t)$, and thus $I_{G-1}(t) < 0$. From Eq. (28) we see that this causes $n_{G-1}(t)$ to grow, and the inaccuracy propagates to the other embryo concentrations.

We mentioned earlier that the growth-rate equations (43a) and (43b) do not apply to the monomer concentration,

$$\frac{d}{dt} n_1(t) \neq e_2 n_2(t) - c_1 n_1(t) \quad (47a)$$

and

$$\frac{d}{dt} n_1(t) \neq -I_1(t). \quad (47b)$$

If a cluster can only change size by gaining or losing single molecules, then the time rate of change of the monomer concentration must depend on the concentrations of all the cluster sizes; if there are $c_2 n_2(t)$ dimers becoming trimers every second, then there are also $c_2 n_2(t)$ monomers depleted per second. This is best illustrated by Fig. 2, which indicates that

$$\frac{d}{dt} n_1(t) = e_2 n_2(t) - c_1 n_1(t) + \sum_{i=1}^{G-1} e_{i+1} n_{i+1}(t) - c_i n_i(t), \quad (48a)$$

or, using Eq. (19),

$$\frac{d}{dt} n_1(t) = -I_1(t) - \sum_{i=1}^{G-1} I_i(t). \quad (48b)$$

The time rate of change of the monomer concentration can be derived in a more quantitative manner by considering the conservation of mass. Let Q be defined as the total number of molecules in the closed nucleating system,

$$Q \equiv V \sum_{i=1}^G i n_i(t), \quad (49)$$

where V is the volume occupied by the system. Since the system is closed, the total number of molecules, Q , is constant:

$$\frac{d}{dt} Q = 0 = V \sum_{i=1}^G i \frac{d}{dt} n_i(t). \quad (50)$$

We can solve this expression for the monomer growth rate,

$$\frac{d}{dt} n_1(t) = - \sum_{i=2}^G i \frac{d}{dt} n_i(t), \quad (51)$$

and then use Eq. (43b),

$$\begin{aligned} \frac{d}{dt} n_1(t) = & -2[I_1(t) - I_2(t)] - 3[I_2(t) - I_3(t)] \\ & -4[I_3(t) - I_4(t)] - \cdots - I_{G-1}(t). \end{aligned} \quad (52)$$

Combining terms, we obtain Eq. (48b).

The correction to the monomer growth rate equation is significant for two reasons. First, because of the coupling in the growth-rate equations (33a), all of the embryo concentrations depend on the monomer concentration; an error like that suggested by Eq. (47a) is propagated to all of the embryos. Secondly, as the steady-state is approached, the currents between concentrations approach the same magnitude; the correct monomer growth-rate equation (48b) will then have a depletion of monomers that is G times as great as that predicted by Eq. (47b) if it were an equality.

IV. A TIME-DEPENDENT SOLUTION TO THE GROWTH-RATE EQUATIONS

The set of coupled differential equations describing the nucleating system, Eqs. (48a) and (43a), can be solved using matrix methods. We first define a column matrix in which the x th row element is the concentration of x -mers, $n_x(t)$,

$$\mathbf{n}(t) \equiv \begin{pmatrix} n_1(t) \\ n_2(t) \\ \vdots \\ n_G(t) \end{pmatrix}. \quad (53)$$

A $G \times G$ matrix is built which contains the condensation and evaporation rates,

$$\mathbf{M} \equiv \begin{pmatrix} -2c_1 & 2e_2 - c_2 & e_3 - c_3 & \cdots & e_{G-1} - c_{G-1} & 0 \\ c_1 & -(c_2 + e_2) & e_3 & \ddots & 0 & 0 \\ 0 & c_2 & -(c_3 + e_3) & \ddots & \vdots & 0 \\ 0 & 0 & c_3 & \ddots & 0 & \vdots \\ 0 & 0 & 0 & \ddots & e_{G-1} & 0 \\ \vdots & \vdots & \vdots & \ddots & -(c_{G-1} + e_{G-1}) & 0 \\ 0 & 0 & 0 & \cdots & c_{G-1} & 0 \end{pmatrix}. \quad (54)$$

This matrix, which we shall call the growth-rate matrix, is singular since the last column only contains zeros. Consider the time derivative of the matrix $\mathbf{n}(t)$,

$$\frac{d}{dt} \mathbf{n}(t) = \begin{pmatrix} \frac{d}{dt} n_1(t) \\ \frac{d}{dt} n_2(t) \\ \vdots \\ \frac{d}{dt} n_G(t) \end{pmatrix} = \begin{pmatrix} e_2 n_2(t) - c_1 n_1(t) + \sum_{i=1}^{G-1} e_{i+1} n_{i+1}(t) - c_i n_i(t) \\ c_1 n_1(t) - (c_2 + e_2) n_2(t) + e_3 n_3(t) \\ \vdots \\ c_{G-1} n_{G-1}(t) \end{pmatrix}. \quad (55)$$

The right-hand side comes from Eqs. (48a) and (43a). But clearly, the right-hand side of Eq. (55) is just $\mathbf{M} \cdot \mathbf{n}(t)$, so we thereby reduce the set of coupled differential equations to one matrix differential equation representing the entire system,

$$\frac{d}{dt} \mathbf{n}(t) = \mathbf{M} \cdot \mathbf{n}(t). \quad (56)$$

In order to obtain the particular solution, we invoke the initial condition that at $t=0$, the vapor is composed of only monomers. The concentration of monomers is given by Eq. (42), so

$$\mathbf{n}(0) = \begin{pmatrix} \frac{p}{kT} \left(1 + \frac{Bp}{kT} \right) \\ 0 \\ \vdots \\ 0 \end{pmatrix}, \quad (57)$$

where p is the pressure of the supersaturated vapor. The particular solution of Eq. (56) with initial condition (57) is the exponential of the growth-rate matrix, \mathbf{M} , times the initial condition column matrix,

$$\mathbf{n}(t) = \exp(\mathbf{M}t) \cdot \mathbf{n}(0), \quad (58)$$

where the matrix exponential is given by²⁵

$$\exp(\mathbf{M}t) = \sum_{j=0}^{\infty} \frac{(\mathbf{M}t)^j}{j!}. \quad (59)$$

With Eq. (58) we have accomplished our goal of obtaining an expression for the time-dependent distribution of each cluster concentration $n_x(t)$. Since computing the exponential of a matrix is a well studied problem,^{25,26} the solution (58) can be calculated. We must now determine the maximum time for which the solution is valid, which we shall call t_F .

In the derivation of the condensation rates for the embryos, the number of monomers was assumed to remain essentially constant. However, if anything is to nucleate, monomers must be depleted; the monomer growth-rate equation (48a) describes the mechanism for this to occur. Furthermore, monomer depletion causes a decrease in the vapor pressure; this lowers the supersaturation ratio, and consequently lowers the nucleation rate. Therefore, we must choose a maximum time for the model that is large enough for the embryo concentrations to fully grow, but small enough that the final concentration of monomers is still approximately equal to the initial concentration, such that the nucleation current is not drastically affected. Miller *et al.*¹² used experimental data to derive an empirical nucleation rate formula which is a function of only the vapor temperature and supersaturation ratio. We have used this formula to calculate the percentage decrease in the nucleation current if, for a given temperature, the supersaturation ratio decreases by 2%; Fig. 3 shows that for supersaturation ratios from 4 to 10, the current decreases 50–70 %, depending on the temperature. Since we assumed that the partial pressure from the monomer concentration remained approximately equal to the total vapor pressure p , $n_1(t)$ is approximately proportional to the supersaturation ratio S ; using Eq. (42) we obtain this proportionality,

$$n_1(t) \approx n_1(0) = \frac{p_{\infty} S}{kT} \left(1 + \frac{Bp_{\infty} S}{kT} \right) \approx \frac{p_{\infty}}{kT} S. \quad (60)$$

Hence, if the monomer concentration decreases by 2%, the supersaturation ratio decreases by 2%, and the nucleation rate decreases by 50–70 %. Although such a decrease in the current appears significant, it is of the same order of magnitude. Since nucleation rates vary over many orders of magnitude for small changes in vapor pressure and temperature, a

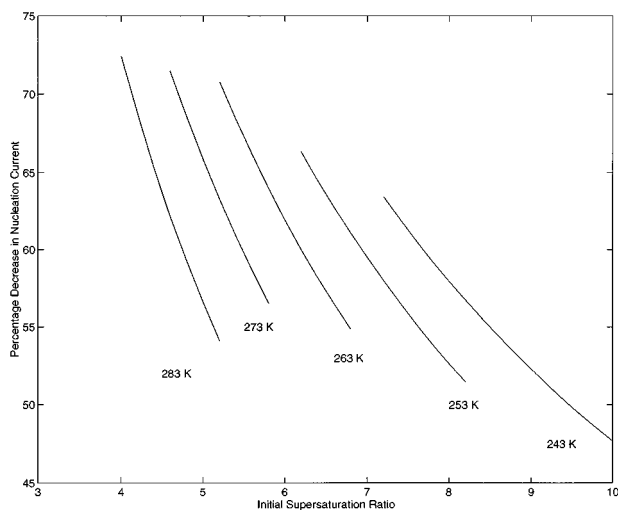


FIG. 3. The effects of a 2% decrease in the supersaturation ratio are shown. Depending on the temperature and initial supersaturation ratio of the water vapor, the nucleation rate decreases approximately 50–70 %.

change of less than 1 order of magnitude is acceptable. We therefore choose t_F , the final time for which our model is valid, to be the time when the monomer concentration has decreased by 2% of its original value; thus,

$$n_1(t_F) \equiv 0.98n_1(0). \quad (61)$$

Of course, the possibility exists that the effect of coagulation and embryo–embryo interactions could become greater than or equal to that of the reactions in Eqs. (1) and (2). Our theory alone could not be applied in such an instance. However, it is beyond the scope of this paper to determine when coagulation processes become dominant, so we will assume that t_F is short enough that Eqs. (1) and (2) are the only significant reactions.

Figures 4 and 5 show distributions of embryo concentrations calculated from Eq. (58) at particular times. The em-

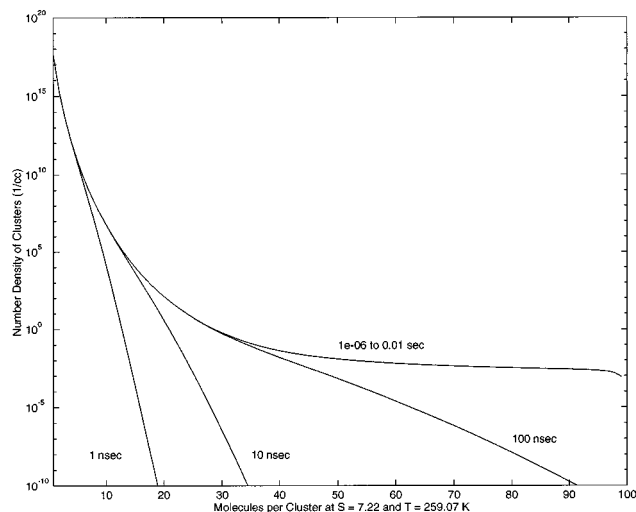


FIG. 4. The distribution of embryo concentrations for water vapor having a supersaturation ratio of 7.22 at 259.07 K evaluated at different times.

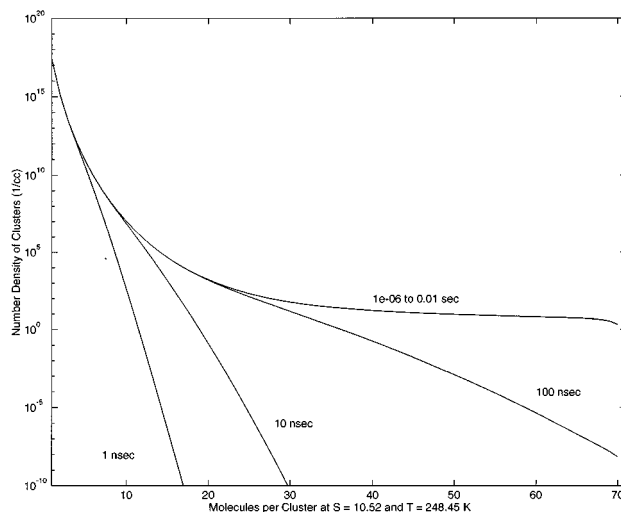


FIG. 5. The distribution of embryo concentrations for water vapor having a supersaturation ratio of 10.52 at 248.45 K evaluated at different times.

bryo concentrations seem to approach the steady state sequentially. Within 1 ns, the number densities of the smallest clusters have stopped growing significantly. As time progresses, successive concentrations appear to reach the steady state, and finally the concentrations with the largest embryos also appear to stop growing. In both cases it seems that the steady state is reached sometime between one hundred nanoseconds and a microsecond; this marks the end of the transient period. We can evaluate the end of the transient period more precisely by using Figs. 6 and 7, which show the time evolution of embryo concentrations of particular sizes. The sequential approach to the steady state is also seen in these figures, more importantly, however, is the fact that the largest clusters require a microsecond before they appear

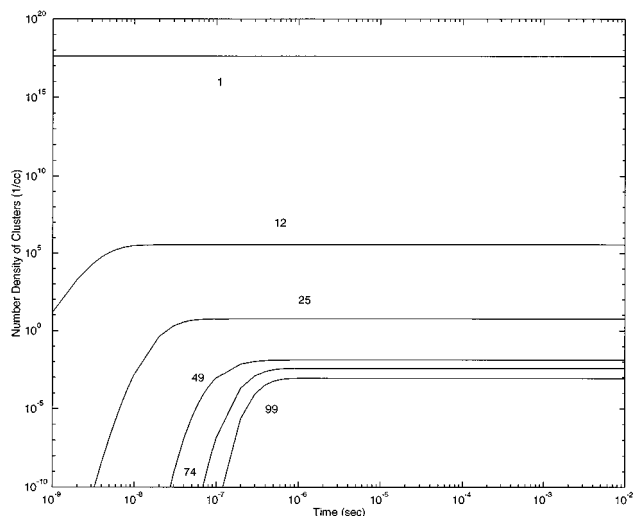


FIG. 6. The time-evolution of specific embryo concentrations is shown for water vapor having a supersaturation ratio of 7.22 at 259.07 K. In descending order from the top of the plot, we see the monomers, 12-mers, 25-mers, 49-mers (the critical size), 74-mers, and 99-mers.

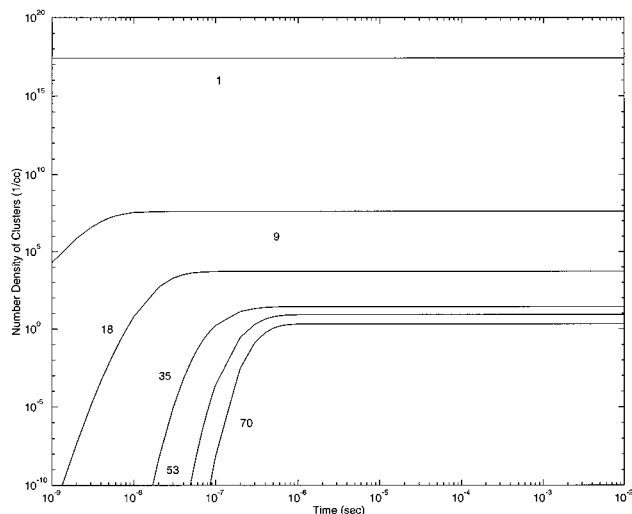


FIG. 7. The time evolution of specific embryo concentrations is shown for water vapor having a supersaturation ratio of 10.52 at 248.45 K. In descending order from the top of the plot, we see the monomers, 9-mers, 18-mers, 35-mers (the critical size), 53-mers, and 70-mers.

steady. Hence, for the two systems modeled, the transient period lasts about a microsecond.

V. REEXPRESSING THE SOLUTION USING EIGENVALUE ANALYSIS

Although Eq. (58) is an exact solution to the embryo growth-rate equations, we cannot predict the physical behavior of a particular embryo concentration by simple inspection; the matrix exponential must be numerically computed. However, we can reexpress this equation using the eigenvalues and eigenvectors of the growth-rate matrix. Eigenvalue analysis illuminates how the embryos approach the steady-state from the transient period, and it allows us to estimate the accuracy of a steady-state approximation.

The horizontal lines in Figs. 6 and 7 are deceptive, because they suggest that the embryo concentrations stop changing. This is not the case; the approach to the steady-state is asymptotic, and the concentrations never completely lose their time dependence. In order to prove this, we must use some auxiliary matrices to reexpress the time dependence of the solution $\mathbf{n}(t)$, Eq. (58). Define a $G \times G$ diagonal matrix \mathbf{L} to contain the eigenvalues, λ_j , of the growth-rate matrix \mathbf{M} ,

$$(\mathbf{L})_{i,j} \equiv \lambda_j \delta_{ij}, \quad i, j \in \{1, 2, \dots, G\}, \quad (62)$$

and define another $G \times G$ matrix \mathbf{V} , the columns of which are the corresponding eigenvectors,

$$\mathbf{M} \cdot \mathbf{V} = \mathbf{V} \cdot \mathbf{L}. \quad (63)$$

In our calculations, we have observed three properties of these eigenvalues. First, the eigenvalues are distinct and real. Secondly, one has the value zero (since \mathbf{M} is singular) and the rest are negative. Thirdly, one of these negative eigenvalues is always significantly smaller in magnitude, i.e., “less negative,” than the others. This will be discussed in greater

detail later. Because the eigenvalues are distinct, the eigenvectors are linearly independent, which allows us to conclude that \mathbf{V} diagonalizes \mathbf{M} . This allows to write \mathbf{M} as

$$\mathbf{V}^{-1} \cdot \mathbf{M} \cdot \mathbf{V} = \mathbf{L} \Rightarrow \mathbf{M} = \mathbf{V} \cdot \mathbf{L} \cdot \mathbf{V}^{-1}. \quad (64)$$

The diagonalization of \mathbf{M} allows us to use Eq. (59) to express the matrix exponential of $(\mathbf{M}t)$ in terms of \mathbf{L} and \mathbf{V} ,

$$\begin{aligned} \exp(\mathbf{M}t) &= \sum_{j=0}^{\infty} \frac{(\mathbf{M}t)^j}{j!} \\ &= \sum_{j=0}^{\infty} \frac{(\mathbf{V} \cdot \mathbf{L} \cdot \mathbf{V}^{-1})^j t^j}{j!} = \mathbf{V} \cdot \left[\sum_{j=0}^{\infty} \frac{(\mathbf{L}t)^j}{j!} \right] \cdot \mathbf{V}^{-1}, \end{aligned} \quad (65)$$

thus

$$\exp(\mathbf{M}t) = \mathbf{V} \cdot \exp(\mathbf{L}t) \cdot \mathbf{V}^{-1}. \quad (66)$$

Let us define a $G \times G$ diagonal matrix, $\mathbf{E}^{\lambda t}$, as follows

$$(\mathbf{E}^{\lambda t})_{i,j} \equiv \delta_{ij} \exp(\lambda_j t), \quad i, j \in \{1, 2, \dots, G\}. \quad (67)$$

Since \mathbf{L} is a diagonal matrix, its matrix exponential is equivalent to taking the exponential of the diagonal elements, thus,

$$\exp(\mathbf{L}t) = \mathbf{E}^{\lambda t}. \quad (68)$$

We can now use Eqs. (66) and (68) to rewrite the time-dependent number density solution, Eq. (58), in terms of the eigenvectors and eigenvalues of the growth-rate matrix,

$$\mathbf{n}(t) = \mathbf{V} \cdot \mathbf{E}^{\lambda t} \cdot \mathbf{V}^{-1} \cdot \mathbf{n}(0). \quad (69)$$

It is convenient to express this matrix equation in terms of its elements,

$$\begin{aligned} [\mathbf{n}(t)]_{x,1} &= \sum_i^G \sum_j^G \sum_l^G (\mathbf{V})_{x,i} (\mathbf{E}^{\lambda t})_{i,j} (\mathbf{V}^{-1})_{j,l} \frac{p}{kT} \left(1 + \frac{Bp}{kT} \right) \delta_{l1} \\ &= \sum_i^G \sum_j^G (\mathbf{V})_{x,i} [\delta_{ij} \exp(\lambda_j t)] (\mathbf{V}^{-1})_{j,1} \frac{p}{kT} \left(1 + \frac{Bp}{kT} \right) \\ &= \sum_i^G (\mathbf{V})_{x,i} \exp(\lambda_i t) (\mathbf{V}^{-1})_{i,1} \frac{p}{kT} \left(1 + \frac{Bp}{kT} \right). \end{aligned}$$

We now have an expression for the single concentration of clusters with x molecules at time t :

$$n_x(t) = \frac{p}{kT} \left(1 + \frac{Bp}{kT} \right) \sum_{i=1}^G (\mathbf{V})_{x,i} (\mathbf{V}^{-1})_{i,1} \exp(-|\lambda_i|t), \quad (70)$$

where $x = 1, 2, 3, \dots, G$ and $0 \leq t \leq t_F$. The exponential term is rewritten as a reminder that the eigenvalues are negative.

The steady-state behavior of the embryo concentrations in Figs. 4, 5, 6, and 7 result from the relative magnitudes of the eigenvalues λ_i in Eq. (70). As mentioned earlier, one of these is equal to zero and the rest are negative. We choose to label the zero eigenvalue λ_G . Additionally, we noted that one

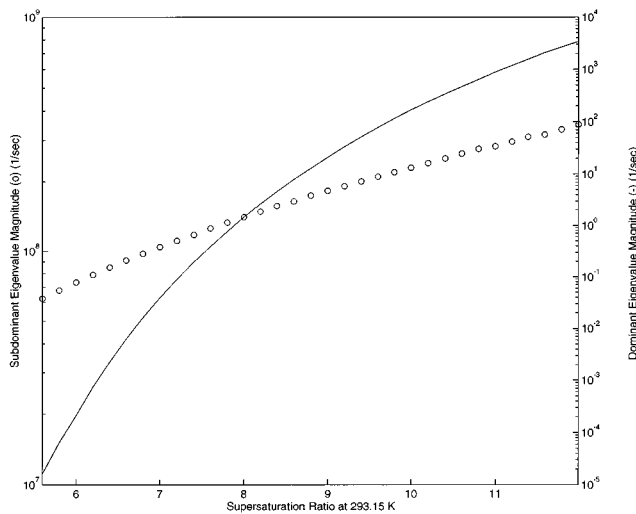


FIG. 8. The absolute values of the subdominant eigenvalue (\circ) and the dominant eigenvalue (line) are shown for a supersaturated water vapor at 293.15 K; the subdominant eigenvalue is the least negative of the λ_i group in Eq. (71). We note that there is a large difference in magnitude between the two, and that the dominant eigenvalue approaches zero as the supersaturation ratio decreases. (The scale for λ_D is on the right and the scale for $\min(|\lambda_i|)$ is on the left.)

of the negative values was much closer to zero than the rest; it will be referred to as the dominant eigenvalue, λ_D . These relationships are summarized as follows,

$$|\lambda_i| \gg |\lambda_D| > \lambda_G = 0, \quad i \neq D \neq G. \quad (71)$$

Figure 8 illustrates this relationship by comparing λ_D to the least negative eigenvalue of the λ_i group.

The relation of the dominant eigenvalue to the steady state can be best understood by considering the time evolution of the cluster concentrations $n_x(t)$, as described by Eq. (70). Because of the relative magnitudes of the eigenvalues, Eq. (71), there may come a time, denoted by $t_{x,D}$, when the λ_i terms in Eq. (70) become negligible compared to the λ_D term; note that the possibility exists for $t_{x,D}$ to be greater than t_F , the maximum time for which our model is valid. Furthermore, it could have different values for different cluster sizes, which is the reason for the x subscript. If $t \gg t_{x,D}$, Eq. (70) will become simpler in form,

$$n_x(t) \approx \frac{p}{kT} \left(1 + \frac{Bp}{kT} \right) [(\mathbf{V})_{x,G}(\mathbf{V}^{-1})_{G,1} + (\mathbf{V})_{x,D}(\mathbf{V}^{-1})_{D,1} \exp(-|\lambda_D|t)], \quad (72)$$

where $t_{x,D} \leq t \leq t_F$. Recalling the structure of the growth-rate matrix, Eq. (54), and noting that λ_G is the zero eigenvalue, it is easy to show that the eigenvector corresponding to λ_G must have zeros for all elements except the last, which must be nonzero,

$$(\mathbf{V})_{x < G, G} = 0, \quad (\mathbf{V})_{G, G} \neq 0. \quad (73)$$

The G -mers only absorb embryos; this results in a nonphysical behavior of growth. Therefore we ignore the G -mers, and rewrite Eq. (72),

$$n_x(t) \approx \frac{p}{kT} \left(1 + \frac{Bp}{kT} \right) (\mathbf{V})_{x,D} (\mathbf{V}^{-1})_{D,1} \exp(-|\lambda_D|t), \quad (74)$$

where $x = 1, 2, \dots, G-1$ and $t_{x,D} \leq t \leq t_F$. We see in Fig. 8 that the dominant eigenvalue rapidly approaches zero as the supersaturation ratio decreases. Thus we can approximate λ_D to be zero, and the approximation becomes better as the supersaturation ratio decreases. This removes the time dependence from Eq. (74),

$$n_x(t) \approx n_x = \frac{p}{kT} \left(1 + \frac{Bp}{kT} \right) (\mathbf{V})_{x,D} (\mathbf{V}^{-1})_{D,1}, \quad (75)$$

where n_x represents the steady-state concentration of x -mers, with $x = 1, 2, \dots, G-1$ and $t_{x,D} \leq t \leq t_F$. Equation (75) is valid only if

$$\exp(-|\lambda_D|t) \approx 1, \quad t \leq t_F. \quad (76)$$

We call this the steady-state condition; if it is satisfied, then after time $t_{x,D}$ the embryo concentrations will essentially lose their time dependence. The closer Eq. (76) is to equality, the more accurate a steady-state approximation will be. Using Eq. (75), we rewrite the x -mer concentration Eq. (70) by pulling the D th term out of the sum and setting λ_D equal to zero,

$$n_x(t) \approx n_x + \frac{p}{kT} \left(1 + \frac{Bp}{kT} \right) \sum_{\substack{i=1 \\ i \neq D}}^{G-1} (\mathbf{V})_{x,i} (\mathbf{V}^{-1})_{i,1} \exp(-|\lambda_i|t), \quad (77)$$

where $x = 1, 2, \dots, G-1$ and $0 \leq t \leq t_F$.

Equation (77) is the final result of our eigenvalue analysis; its form (which consists of a time-independent steady-state term added to a time-dependent transient term) allows us to determine the general physical behavior of the embryos by simple inspection. Given the form of Eq. (77), it is clear that an x -mer concentration approaches the steady state asymptotically during the nucleation process. Furthermore, knowing that the time-dependent transient portion becomes negligible for $t \gg t_{x,D}$, we can deduce that $t_{x,D}$ is the duration of the transient period for the x -mers. Finally, by evaluating the steady-state condition, Eq. (76), for a particular growth-rate matrix, we can determine the relative accuracy of a steady-state approximation. McDonald suggested that evaluating the steady-state nucleation current is analogous to finding the steady-state heat flux through a slab which has a constant known temperature at each face.⁷ Equation (77), having the same form as the heat-flux solution, supports his claim.

VI. COMPARISONS BETWEEN THEORY AND EXPERIMENT

Equations (58) and (70) are exact and equivalent solutions for the growth-rate equations (43a) and (48a). For physically realistic problems the growth-rate matrix is large, e.g., 100×100 for water vapor with a supersaturation ratio equal to 7.22 at 259.07 K. Obtaining all of the eigenvalues and eigenvectors is certainly possible, but it is nontrivial.

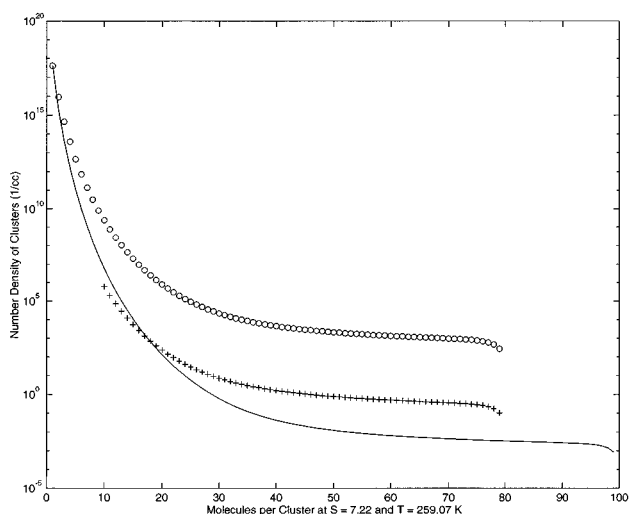


FIG. 9. We compare the embryo concentration steady-state distributions of this work (line), Abraham (+), and Gillespie (O) for water vapor having a supersaturation ratio of 7.22 at 259.07 K.

Furthermore, as the size of eigenvector matrix \mathbf{V} increases, it becomes ill-conditioned and approaches singularity; this complicates the calculation of \mathbf{V}^{-1} . Sometimes the addition of terms in Eq. (70) introduces significant round-off problems. Therefore, although Eq. (70) is theoretically advantageous for deducing embryo concentration behavior, there are many chances for numerical error to ruin the results. We have found that using Eq. (58), which involves calculating the exponential of the growth-rate matrix, is numerically more reliable and consistent; thus, we have used it for computing the results which we shall refer to. We have limited our calculations and comparisons to systems of supersaturated water vapor.

Figures 9 and 10 compare the steady-state distributions evaluated using Eq. (58) at 1 ms to those of Abraham¹⁶ and

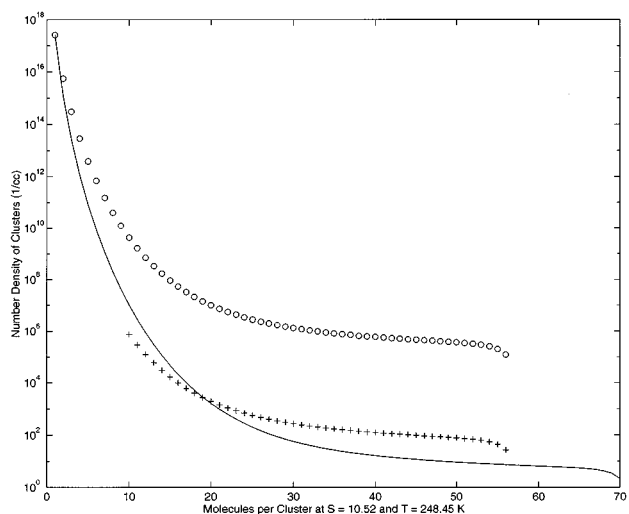


FIG. 10. We compare the embryo concentration steady-state distributions of this work (line), Abraham (+), and Gillespie (O) for water vapor having a supersaturation ratio of 10.52 at 248.45 K.

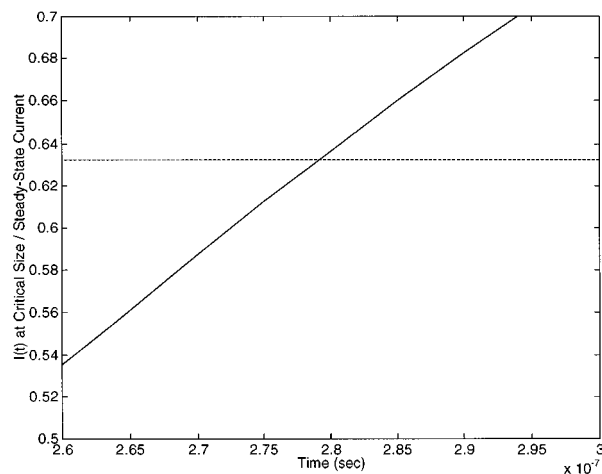


FIG. 11. The nucleation current at the critical size is divided by the steady-state current, and the time evolution of this ratio is shown (solid line). The dashed line marks the ratio's value at 0.632. The time lag is then approximated as the moment when the solid and dashed lines intersect. The system considered is water vapor having a supersaturation ratio of 4.91 at 263.2 K.

Gillespie.²⁴ Abraham's approach follows that of the classical theory, in which the classical free energy, the Szilard boundary condition, and the constrained equilibrium Boltzmann distribution are employed. He obtained figures similar to 6 and 7 by using a nonlinear integration routine to numerically solve the growth-rate equations; it is interesting to note that Eq. (58) and the model of Abraham predict the same general time evolution for the embryos. He did not obtain a closed form expression for the time dependence of the cluster concentrations, but did derive a steady-state distribution that agrees with his numerical integration results; we have used this expression for our comparison. Gillespie also derived a steady-state distribution of embryos, which we have used. Although Gillespie did not explicitly present a solution for the time evolution of cluster concentrations, he derived a time-dependent matrix expression for the probability that an embryo, initially a monomer, would be an x -mer at time t . He proved that one could obtain the average number of x -mers at time t by simply multiplying this probability by the total number of embryos (including monomers); unfortunately, he did not perform the necessary calculations to obtain the time-dependent distributions. We did the calculations, however, and found that the embryo concentrations again exhibited the same general behavior as in Figs. 6 and 7, and that they relaxed into values that agreed with Gillespie's steady-state expression. Figures 9 and 10 show us that Abraham's results predict more medium-sized and large clusters than our model, and that the Gillespie model predicts the most clusters in the comparison.

Many theories²⁷⁻³⁰ have been developed to estimate the time it takes for the nucleating system to significantly approach the steady state. This time lag is usually defined as the moment when the current at the critical size reaches $1 - 1/e$, approximately 63.2% of the steady-state current. Having a time-dependent expression for the embryo concentrations makes this estimation a trivial matter. Figure 11

shows that for water vapor having a supersaturation ratio of 4.91 and at a temperature of 263.2 K, the time lag is approximately 0.28 ms. Abraham¹⁸ (Table 5.6 of Ref. 18) made similar calculations for the same system using two different definitions of the time lag, his results were 0.46 and 0.43 ms. He also used the models of Wakeshima,²⁷ which predicted 0.16 ms; Collins,²⁸ which predicted 0.49 ms; Feder *et al.*,²⁹ which predicted 0.98 ms; and Andres and Boudart,³⁰ which predicted 0.55 ms.

We can check the accuracy of our results by comparing our steady-state nucleation rates with experimental data. This is convenient, since most experimentalists have been concerned with measuring nucleation rates, rather than distributions of embryo concentrations. Viisanen *et al.*¹³ present data that shows acceptable agreement with the work of Miller *et al.*;¹² we will use the expansion chamber results of both Viisanen *et al.* and Miller *et al.* for our subsequent comparisons. Our rates will be calculated by using the definition of the nucleation current, Eq. (19), at the critical size and by evaluating Eq. (58) at 1 ms; 1 ms is chosen because it is enough time for the embryo concentrations to sufficiently approach their steady-state values and it is the general duration of a nucleation pulse in the expansion chamber experiments of Viisanen *et al.* Using the current at the critical size is purely an arbitrary choice, since the currents at each x value are approximately equal once they are steady. The thermodynamic parameters (saturation vapor pressure, the second virial coefficient, etc.) were calculated using the functions presented by Dillmann and Meier.

For the system having supersaturation ratio of 7.22 and a vapor temperature of 259.07 K (Fig. 9) Viisanen *et al.* measured the nucleation rate to be $1.9e+05$ embryos/cc/sec; the empirical fitting function of Miller *et al.* predicted a value of $5.47e+05$ embryos/cc/sec. Using Abraham's steady-state current equation (which is essentially the classical Becker and Döring nucleation current), we calculate that Abraham's model predicts $5.08e+07$ embryos/cc/sec. Gillespie's steady-state current expression yields a nucleation rate of $1.38e+11$ embryos/cc/sec. Our model predicts a value of $7.22e+05$ embryos/cc/sec.

The system with a vapor temperature of 248.45 K and a supersaturation ratio of 10.52 (Fig. 10) is beyond the range of the Miller *et al.* fitting function, so it will not be used here. Although Viisanen *et al.* measure the current to be $1e+08$ embryos/cc/sec, the models of Abraham and Gillespie predict its value at $6.34e+09$ and $2.92e+13$ embryos/cc/sec, respectively. Our model yields a nucleation rate of $9.06e+08$ embryos/cc/sec.

Note that in both systems, the nucleation current calculated from Eqs. (58) and (19) was significantly closer to the experimentally measured values than that predicted by Abraham or Gillespie. We will therefore assume that the distributions of cluster concentrations computed from Eq. (58) are also more accurate.

Two cases of agreement are not enough to assume a general trend of accuracy, however. We now make a more general comparison with theory and experiment over a wide range of temperatures and supersaturations. In addition to

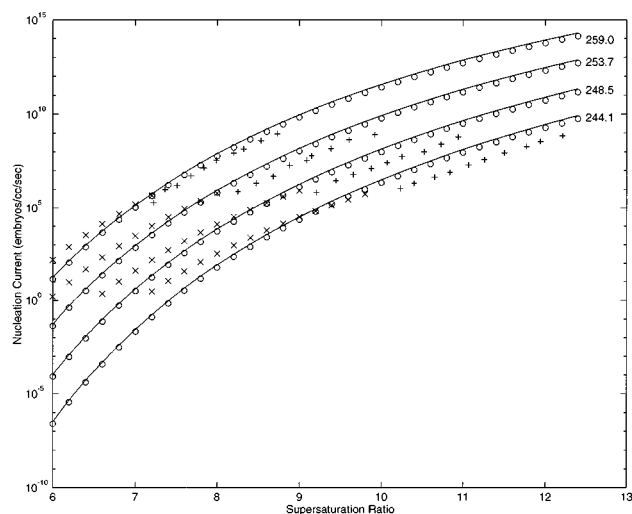


FIG. 12. The nucleation rates predicted by this work (line) are compared with the predictions of the Laaksonen *et al.* theory (O) and the experimental measurements of Miller *et al.* (X) and Viisanen *et al.* (+). The temperatures corresponding to the data are given in Kelvin. A supersaturated water vapor is considered.

using the experimental data of Miller *et al.* and Viisanen *et al.*, we will compare our nucleation rates with those predicted by Laaksonen *et al.*¹⁴ We choose Laaksonen *et al.* because their theory produces currents that are in excellent agreement with experimental data for many substances, including water, n -nonane, and the lower alcohols. Unfortunately, Laaksonen *et al.* did not present an expression for the nucleation rate within their study. Since they were modifying the theory of Dillmann and Meier, we have used Dillmann and Meier's general expression for the current,

$$I = C_{x_c} \frac{N_{x_c}^E}{V} \left(\frac{-1}{2\pi kT} \frac{\partial^2 \Delta G_x}{\partial x^2} \right)^{1/2} \Big|_{x=x_c}, \quad (78)$$

where C_{x_c} is Dillmann and Meier's condensation rate at the critical size. We have combined Eqs. (38) ($\tau=0$) and (39) with Eq. (78) to obtain the Laaksonen *et al.* nucleation currents. The results of this comparison are given in Fig. 12. We see that our predictions for the current agree quite well with the values obtained from the Laaksonen *et al.* theory. The agreement with experiment is also very good, remaining within 1 order of magnitude. Note that the curves implied by our predictions are parallel to those implied by the data of Viisanen *et al.*, but not to those of Miller *et al.* Viisanen *et al.* found that the Miller *et al.* fitting function had slightly too much curvature, and considered it valid only for rates between $1e+02$ and $1e+05$. This is a narrower range than we have used in Fig. 12, and our agreement with Miller *et al.* is improved if we only consider the data within that range. In order to make sure that one millisecond is less than t_F for this data set, we have calculated the monomer depletion ratio, which is the ratio of the time-dependent monomer concentration to its initial value; see Fig. 13. These ratios stay well above the limit of 0.98 set forth by Eq. (61). An interesting aspect of the monomer depletion ratios in Fig. 13 is

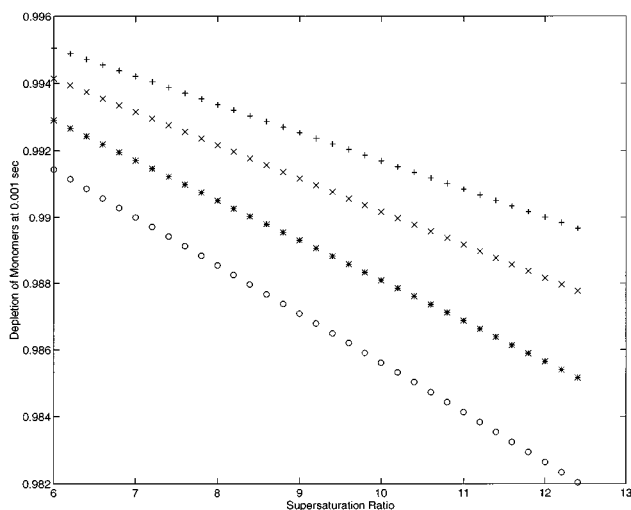


FIG. 13. The monomer depletion ratio at 1 ms is plotted vs the supersaturation ratio for supersaturated water vapor at 259.0 K (○), 253.7 K (*), 248.5 K (×), and 244.1 K (+). The monomer depletion ratio is defined as the ratio of the monomer concentration, at a given time, to the initial monomer concentration.

that their values seem to decrease linearly as the supersaturation ratio increases. Furthermore, the rate of decrease seems to depend on the temperature. For a saturated vapor, which is in equilibrium, the monomer depletion ratio must equal 1. We can use this fact to guess at a general expression for the lines implied by the data points in Fig. 13,

$$\left. \frac{n_1(t)}{n_1(0)} \right|_{t=0.001} \approx -|M(T)|(S-1) + 1. \quad (79)$$

It is unknown if the temperature-dependent slope, $M(T)$, has any additional physical meaning besides the rate at which the monomer depletion ratio decreases. Figure 14 confirms that

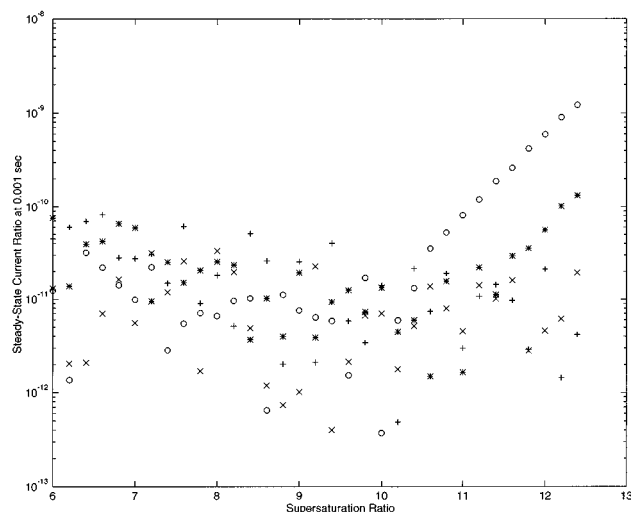


FIG. 14. The steady-state current ratio at 1 ms is plotted vs the supersaturation ratio for supersaturated water vapor at 259.0 K (○), 253.7 K (*), 248.5 K (×), and 244.1 K (+). The steady-state current ratio is defined by Eq. (80).

the currents for this data set are close to their steady-state values. The steady-state current ratio, $R(t)$, is defined as,

$$R(t) \equiv \frac{|I_{x_C}(t) - I_{G-2}(t)|}{I_{x_C}(t)}. \quad (80)$$

If the embryo concentrations are approximately in their steady state, this ratio should approach zero. We see that $R(t)$, evaluated at 1 ms, ranges from $1e-09$ to $1e-13$, so the currents have indeed become steady.

VII. CONCLUDING REMARKS

We have presented a time-dependent model for the homogeneous nucleation process, and derived a time-dependent solution, Eq. (58), to the coupled growth-rate differential equations for molecular cluster concentrations. We have also corrected the monomer concentration growth-rate equation so that it allows for the gain and loss of molecules by each cluster population. Although our approach is basically kinetic, our evaporation rate uses the refinements to the Dillmann and Meier theory presented by Laaksonen *et al.*¹⁴ and Ford *et al.* This enables us to account for cluster size-dependent surface tension variations. Additionally, our condensation rate incorporates the translational motion of each embryo, rather than assuming that monomers are the only moving bodies. A different but equivalent solution to the growth-rate equations is formed by expressing the exponential of the growth-rate matrix in terms of its eigenvalues and eigenvectors. This form is theoretically advantageous because we find that the relationship between the relative magnitudes of the eigenvalues governs the embryos' transition from the initial transient period to the steady state. The magnitude of the dominant eigenvalue also allows us to formulate the steady-state condition, Eq. (76), which predicts the general accuracy of approximating an embryo concentration as being steady.

A useful feature of our development is that it can be applied to almost any nucleation rate theory in order to obtain the time-dependent behavior of the cluster populations. The model requires an expression for the Gibbs free energy to be substituted into Eq. (22). We have applied the free energies of Dillmann and Meier, Delale and Meier, and Laaksonen *et al.*, and in each case we obtain nucleation rates approximately equal to those calculated by each theory; the agreement is approximate primarily because our condensation rate differs from the applied theory's. If the condensation rates are made to be equivalent, however, we find the agreement to be practically exact. Thus our calculated time-dependent cluster growth that is associated with the applied theory can be considered accurate.

For supersaturated water vapor, the steady-state distribution of embryos predicted by Eq. (58) has significantly different values than that predicted by Abraham or Gillespie. However, the nucleation current associated with our distribution is closest to experimental data. A comparison over a wide range of water vapor supersaturation ratios and temperatures shows that the currents calculated from Eq. (58) agree with the measurements of Miller *et al.* and Viisanen

et al.; furthermore, our predictions are in excellent agreement with those of Laaksonen *et al.*,¹⁴ which have been experimentally verified for many different substances and conditions. At present our predictions are limited to water vapor; further comparisons involving other substances, such as ethanol, *n*-nonane, etc., are needed.

The time-dependent expression for the cluster concentrations makes it easy to compute quantities such as the time lag for the approach to the steady state. For the one example considered, our result was midway between those of Wakeshima and Abraham. Certainly, a broad comparison of the time lags predicted by this and other theories, as well as some type of experimental verification, is needed.

Although our solution to the growth-rate equations is accurate, our model would be improved physically if the constant monomer assumption were eliminated. This would result in a time-dependent condensation rate,

$$c_x(t) = \xi_x n_1(t), \quad (81)$$

where

$$\xi_x \equiv \frac{c_x}{n_1(0)}. \quad (82)$$

In this case, the coupling of the growth-rate equations becomes more complicated,

$$\begin{aligned} \frac{d}{dt} n_1(t) = & e_2 n_2(t) - \xi_1 [n_1(t)]^2 + \sum_{i=1}^{G-1} e_{i+1} n_{i+1}(t) \\ & - \xi_i n_1(t) n_i(t) \end{aligned} \quad (83)$$

and

$$\begin{aligned} \frac{d}{dt} n_x(t) = & \xi_{x-1} n_1(t) n_{x-1}(t) - [\xi_x n_1(t) + e_x] n_x(t) \\ & + e_{x+1} n_{x+1}(t). \end{aligned} \quad (84)$$

Solving these new equations is probably not worth the extra effort, since corrections to our values are expected to be minor.

ACKNOWLEDGMENTS

One of us (T. Olson) received a research grant from the National Science Foundation which is gratefully acknowledged. Both of us acknowledge partial support by NASA Grant No. NAGW-3525. The authors also wish to thank Alejandro Garcia for many helpful discussions.

- ¹R. Becker and W. Döring, *Ann. Phys. (Leipzig)* **24**, 719 (1935).
- ²L. Farkas, *Z. Phys. Chem. Abt. A* **125**, 236 (1927).
- ³J. Frenkel, *Kinetic Theory of Liquids* (Dover, New York, 1955).
- ⁴M. Volmer and A. Weber, *Z. Phys. Chem.* **119**, 277 (1926).
- ⁵J. B. Zeldovich, *J. Exp. Theor. Phys.* **12**, 525 (1942).
- ⁶J. E. McDonald, *Am. J. Phys.* **30**, 870 (1962).
- ⁷J. E. McDonald, *Am. J. Phys.* **31**, 31 (1963).
- ⁸C. T. R. Wilson, *Philos. Trans. A* **189**, 265 (1897).
- ⁹C. F. Powell, *Proc. R. Soc. London, Ser. A* **119**, 553 (1928).
- ¹⁰M. Volmer and H. Flood, *Z. Phys. Chem. A* **170**, 273 (1934).
- ¹¹P. E. Wagner and R. Strey, *J. Phys. Chem.* **85**, 2694 (1981).
- ¹²R. C. Miller, R. J. Anderson, J. L. Kassner, Jr., and D. E. Hagen, *J. Chem. Phys.* **78**, 3204 (1983).
- ¹³Y. Viisanen, R. Strey, and H. Reiss, *J. Chem. Phys.* **99**, 4680 (1993).
- ¹⁴A. Laaksonen, I. J. Ford, and M. Kulmala, *Phys. Rev. E* **49**, 5517 (1994).
- ¹⁵A. Dillmann and G. E. A. Meier, *J. Chem. Phys.* **94**, 3872 (1991).
- ¹⁶F. F. Abraham, *J. Chem. Phys.* **51**, 1632 (1969).
- ¹⁷C. F. Wilcox, Jr., and S. H. Bauer, *J. Chem. Phys.* **94**, 8302 (1991).
- ¹⁸F. F. Abraham, *Homogeneous Nucleation Theory* (Academic, New York, 1974), pp. 80–101.
- ¹⁹G. A. Bird, *Molecular Gas Dynamics* (Clarendon, Oxford, 1976), pp. 67–69.
- ²⁰J. L. Katz and H. Wiedersich, *J. Colloid Interface Sci.* **61**, 351 (1977).
- ²¹A. Laaksonen, V. Talanquer, and D. Oxtoby, *Annu. Rev. Phys. Chem.* **46**, 489 (1995).
- ²²I. J. Ford, A. Laaksonen, and M. Kulmala, *J. Chem. Phys.* **99**, 764 (1993).
- ²³C. F. Delale and G. E. A. Meier, *J. Chem. Phys.* **98**, 9850 (1993).
- ²⁴D. T. Gillespie, *J. Chem. Phys.* **74**, 661 (1981).
- ²⁵G. H. Golub and C. F. Van Loan, *Matrix Computations*, 2nd Ed. (Johns Hopkins University, Baltimore 1989), pp. 555–560.
- ²⁶C. Moler and C. Van Loan, *SIAM Review* **20**, 801 (1978).
- ²⁷H. Wakeshima, *J. Chem. Phys.* **22**, 1614 (1954).
- ²⁸F. C. Collins, *Z. Electrochem.* **59**, 404 (1955).
- ²⁹J. Feder, K. C. Russell, J. Lothe, and G. M. Pound, *Advan. Phys.* **15**, 111 (1966).
- ³⁰R. P. Andres and M. Boudart, *J. Chem. Phys.* **42**, 2057 (1965).